

Efficient Propagation of Uncertainties in Supply Chains: Time Buckets, L-leap and Multi-Level Monte Carlo

Nai-Yuan Chiang, Yiqing Lin, Quan Long*

*United Technologies Research Center
411 Silver Lane, East Hartford, CT, USA*

Abstract

Uncertainty quantification of large scale discrete supply chains can be prohibitive when a large number of events occur during the simulated period and discrete event simulations (DES) are costly. We present a time bucket method to approximate and accelerate the DES of supply chains. Its stochastic version, which we call the L(logistic)-leap method, can be viewed as an extension of the D-leap method [3] developed in the chemical engineering community for the acceleration of stochastic DES of chemical reactions. The L-leap method updates the system state vector at discrete time points and imposes constant production rates and Boolean values associated with the logic of a supply chain during each time bucket. We propose to use Multilevel Monte Carlo (MLMC) to efficiently propagate the uncertainties in a supply chain network, where the levels are naturally defined by the sizes of the time buckets of the simulations. The MLMC approach can be 10 times faster than the standard Monte Carlo (MC) method which computes the samples exactly using DES. We demonstrate the efficiency and accuracy of our methods using five material flow examples. The first three examples demonstrate the performance of the time bucket method in both deterministic and stochastic settings for a simple push system, a simple pull system and a complex pull system with features like back-ordering, priority-production and transportation. The fourth example considers multilevel uncertainty propagation of the push system under parametric uncertainties. The fifth example considers multilevel uncertainty propagation of the complex pull system under both parametric and stochastic uncertainties.

Keywords: Uncertainty modeling; Discrete event simulation; Multilevel Monte Carlo; L-leap; Supply chain

1. Introduction

Supply chains are coordinated flows of materials from the suppliers to the locations where they are supposed to be consumed. As one of the major supply chain simulation methodologies, DES concerns the modeling of a system as it evolves over time by a representation in which the state variables change

*Corresponding author

Email addresses: chiangn@utrc.utc.com (Nai-Yuan Chiang), liny@utrc.utc.com (Yiqing Lin), longq@utrc.utc.com (Quan Long)

instantaneously at distinct points in time [19]. The method is commonly used to analyze complex processes that are challenging with closed-form analytical methods. DES is widely used for supply chain management analysis such as manufacturing process and logistics planning [16, 21, 34]. Simulations enable the design of the supply chain, and the evaluation of supply chain management prior to implementation of the system to perform what-if analysis [31].

A DES model is rarely run only once. Multiple simulation runs are usually required for various purposes. As input parameters, e.g., processing time of a product, are often random variables, multiple runs with different realizations of the random input variables are required in order to obtain statistically meaningful outputs. Furthermore, if a sensitivity analysis is applied on a simulation model to select input variables that have the largest impact on response variables, another layer of multiple runs are needed to vary input parameters such as different distributions of processing times [20, 23]. Optimization is another technique that can be combined with DES to define optimal input control variables, e.g., production capacity. Each iteration of an optimization requires multiple simulation runs for a set of system parameters [11, 17, 26, 32].

In summary, a large amount of DES runs are often required for an analysis task. As the scale of supply chains grows large, for example, due to globalization and inter-enterprise collaboration [2, 28], some simulation models may take hours to complete one run. Therefore, the time to perform analysis with thousands, sometimes hundreds of thousands, of DES runs for a complex supply chain can be prohibitively long when standard MC is used.

As an approximation of DES, the full simulated time can be divided into periods of given time buckets, Δt . Time bucket based simulation does not model the occurrence of each event, instead, it counts the number of events happened in each time bucket, at the end of which the system state is updated using the model equations. Therefore, in this approach, events can be considered to occur instantaneously at the beginning of a period [31]. Note that our terminology-“time bucket” is consistent with the supply chain literature [22, 29, 18], while Δt can be equivalently denoted by “time interval”, “time leap”, etc. The size of the time bucket can be defined either as a fixed value or in a time-dependent fashion. When the size of a time bucket is small enough that each bucket has at most one event, then the model is equivalent to DES. The advantage of the time bucket method is that it is more scalable compared with DES when the size of a time bucket is relatively large. The disadvantage is that due to the aggregation of multiple events, some interactions between events are lost, thus the model is not as accurate as DES, and is less commonly used. The Tau-leap method [14, 6, 24, 7] is essentially a stochastic time bucket method that has been widely used to accelerate the simulations of chemical reactions modeled by continuous time Markovian processes. Rather than simulating every discrete event, Tau-leap method simulates the stochastic change of the system states at discrete time points using constant propensity function to simulate the number of processes happening during a time bucket. Although the simulation results are biased due to the time buckets, significant acceleration can be achieved under acceptable tolerance. Recently, the D-leap method

has been proposed to accelerate the simulations of delayed chemical reactions [3] by introducing a queue of reactions to take account of the delays.

Our innovations are as follows. First, we extended the D-leap method to consider features of supply chain logistic networks. The resulting *L(logistic)-leap* method is able to consider production time, transportation time, limited capacity, pull system and priority production. Secondly, we used MLMC method based on time buckets to propagate the uncertainties in a supply chain, where most of the computational work is shifted from the expensive models, e.g., DES, to the cheap models defined by large time buckets. Similar to applying the multilevel Tau-leap method to chemical reactions for better scalability [1, 25], the proposed approach is able to match the model accuracy of DES while overcoming its scalability limitation with the help of MLMC.

Section 2 describes the accelerated approximation of DES using the time bucket method and the detailed algorithms for the simulation of supply chain features. Section 3 introduces the L-leap method which specifically is a time bucket method for simulating logistic systems driven by stochastic processes. Section 4 presents an MLMC method in which the samples are drawn from populations simulated using different sizes of time buckets. In Section 5 we show the accuracy and gain in computation speed using extensive examples. The first example concerns push system where the production does not depend on orders. The second example is a pull system with periodic orders of the final products. The third example is a pull system with mixed orders of the spare parts and the final products, which also considers transportation delays. The fourth example considers the uncertainty propagation of the push system under parametric uncertainties. The fifth example considers the uncertainty propagation of the pull system under both parametric and stochastic uncertainties. The quantities of interests are the final delivery time of fixed amount of orders and the number of deliveries over a specified time period. We show that the error of the predictive simulations with respect to (w.r.t.) the true solution provided by DES diminishes as we decrease the size of the time bucket. We achieve a factor of 10 speed up in computing the expected quantities of interest using an MLMC method based on the time buckets and L-leap, comparing to the standard MC approach.

2. Time bucket approximation of DES

Supply chains transport materials from the suppliers to the places where they are consumed. The raw materials usually get consumed and transformed into some intermediate products. To clarify the notation, raw materials, intermediate products and final products are treated as different parts in this paper, and a unique symbol is assigned to each part. We define a part set \mathbb{P} of all the parts, $\mathbb{S} \subset \mathbb{P}$ for all the supplies of raw materials and $\mathbb{E} \subset \mathbb{P}$ for all the final products. The DES simulates the events associated with discrete mass flows with limited capacities, specifically the production rate of each process is bounded from above.

A supply chain can be defined by a set of n processes, each of which can be described as follows

$$\{\alpha_{ij}\hat{p}_{ij}|j = 1 : \hat{n}_i\} \rightarrow \{\beta_{ik}\tilde{p}_{ik}|k = 1 : \tilde{n}_i\} \quad i = 1, \dots, n, \quad (1)$$

where for each process i , \hat{n}_i is the number of consumed parts, \tilde{n}_i is the number of produced parts, \hat{p}_{ij} denotes the j^{th} consumed part and \tilde{p}_{ik} denotes the k^{th} produced part. We use α_{ij} and β_{ik} as the integer weights corresponding to parts \hat{p}_{ij} and \tilde{p}_{ik} , respectively. That is, if process i happens once, it consumes α_{ij} part \hat{p}_{ij} and will produce β_{ik} part \tilde{p}_{ik} . From the definition of the set \mathbb{P} , it contains all the parts in the system, and hence we have $\mathbb{P} = \{\hat{p}_{ij}\} \cup \{\tilde{p}_{ik}\}$, for all i, j and k . Similarly, we have $\mathbb{S} = \{\hat{p}_{ij}\} \setminus \{\tilde{p}_{ik}\}$ and $\mathbb{E} = \{\tilde{p}_{ik}\} \setminus \{\hat{p}_{ij}\}$ for all i, j and k . We denote $\mathbf{x} \in \mathbb{R}^{|\mathbb{P}|}$ as the state vector recording the number of parts, where $|\cdot|$ denotes the set cardinal. Note that the mapping $\{x\} \rightarrow \mathbb{P}$ is bijective, where $\{x\}$ is the set of the components of \mathbf{x} . Based on the definitions of \hat{p}_{ij} and \tilde{p}_{ik} , we have $x_{\hat{p}_{ij}}$ as the number of the j^{th} part consumed in the i^{th} process, and, similarly, $x_{\tilde{p}_{ik}}$ is the number of the k^{th} part produced in the i^{th} process. For clarity, in the following contexts we use \hat{x}_{ij} and \tilde{x}_{ik} to denote these quantities. At time t , the process occurs at a rate $\lambda_i(t)$ which is given by

$$\lambda_i(t) = \begin{cases} \lambda_i^{max} & \text{if } \min_j \{\hat{x}_{ij}(t) - \alpha_{ij}\lambda_i^{max}\Delta t\} \geq 0 \\ \min_j \left\{ \frac{\lfloor \frac{\hat{x}_{ij}(t)}{\alpha_{ij}} \rfloor}{\Delta t} \right\} & \text{otherwise} \end{cases}, \quad (2)$$

where λ_i^{max} is the maximum production rate (capacity) associated with the i^{th} process, Δt is the size of the time bucket, $\lfloor x \rfloor = \max\{m \in \mathbb{Z} | m \leq x\}$ is the floor function. The first equation in (2) shows that the process can achieve its maximum rate if all its materials have enough inventory in this time bucket, otherwise, the rate λ_i is reduced to the value which prevents negative values of the consumed materials during this time bucket. Equation (2) denotes a deterministic production rate, while other alternatives are possible. For example, the consumption rate λ_i in (2) can be modeled by incorporating the expected arrivals of the consumed parts [10], i.e., when one part, e.g., \hat{p}_{ij} , is out of stock, its availability in the next time bucket may be estimated by checking the scheduled productions in the preceding processes over this time bucket. If the number of scheduled productions plus the current inventory is larger than $\lambda_i^{max}\Delta t$, the maximum capacity, λ_i^{max} , can still be achieved. Otherwise, the consumption rate λ_i can be adjusted to match the summation of the expected arrival of \hat{p}_{ij} and its current inventory. However, we use (2) in our approach since it is more likely preventing the negative inventory value of \hat{p}_{ij} . Note that the difference between our approach with the discussed alternative would be asymptotically small w.r.t. Δt .

It is also worth mentioning that if a single part can be consumed by multiple processes, we need to define

a distribution policy among the processes. In this case, one way to modify equation (2) is as follows

$$\lambda_i(t) = \begin{cases} \lambda_i^{max} & \text{if } \min_j \{ \hat{x}_{ij}(t) - \sum_{\{i' \mid \exists \hat{p}_{i'j'} = \hat{p}_{ij}\}} \alpha_{i'j'} \lambda_{i'}^{max} \Delta t \} \geq 0 \\ \min_j \left\{ \left\lfloor \frac{\hat{x}_{ij}(t)}{|\{i' \mid \exists \hat{p}_{i'j'} = \hat{p}_{ij}\}| \cdot \alpha_{ij}} \right\rfloor \right\} & \text{otherwise} \end{cases}, \quad (3)$$

which assumes that part \hat{p}_{ij} is evenly consumed by all the processes requiring it.

The time bucket simulation of a supply chain process can be split into two major phases: 1) material consumption: each process consumes the necessary parts instantaneously according to its production rate - $\lambda_i(t)$. 2) delayed production: due to the required processing time (lead time) in each process, we consider all the productions require delays after materials have been instantaneously consumed. Note that our consumption-delayed-production framework is inspired by the D-leap method for delayed chemical reaction network simulation in [3]. Importantly, in the context of logistics, we enriched the D-leap method with several salient features of supply chains: transportation, order-driven production (pull system), and priority production. The consumption-production phases are tightly correlated due to the mass-conservation of the material flow in the supply chain network.

2.1. Consumption

The consumption of parts happening in each time bucket is instantaneously taken into account at the beginning of every time bucket. In each time bucket Δt , the total number of triggered processes i reads

$$\Delta C_i(t) = \lambda_i(t) \Delta t. \quad (4)$$

The state vector is then updated by the following equation

$$\hat{x}_{ij}(t) = \hat{x}_{ij}(t - \Delta t) - \alpha_{ij} \Delta C_i(t), \quad j = 1, \dots, \hat{n}_i. \quad (5)$$

For the sake of conciseness, we omit variable t and use ΔC_i instead of $\Delta C_i(t)$ in the remainder of this paper.

As mentioned previously, executions of the process lead to corresponding number of delayed productions via (4). At each time point, we check if the executions should be completed or not, and estimate the quantity of completions. In the implementation, a queue structure is created to store the necessary information, i.e., the index of the delayed process- d_{n_q} , where $n_q = 1, \dots, N_q$, N_q is the number of process batches in the queue, the number of the delayed processes- $Q_{n_q}^{delay}$, the earliest time of the production being completed- $t_{n_q}^s$, the time span between the earliest and the latest times of the production being completed- $t_{n_q}^{span}$.

The earliest production time and the latest production time of the ΔC_i processes can be computed as follows

$$t_{n_q}^s = t + \hat{t}_{d_{n_q}}^{min}, \quad (6)$$

$$t_{n_q}^{span} = t + \Delta t + \hat{t}_{d_{n_q}}^{max} - t_{n_q}^s = \Delta t + \hat{t}_{d_{n_q}}^{max} - \hat{t}_{d_{n_q}}^{min}, \quad (7)$$

where \hat{t}_i^{min} and \hat{t}_i^{max} are the minimum and maximum lead times for each process i correspondingly. The definitions are schematically shown in Figure 1.

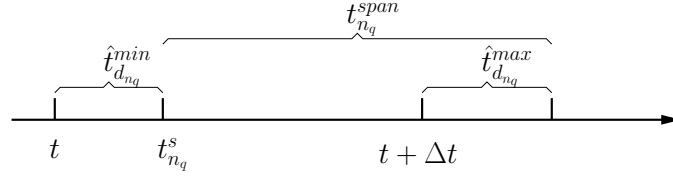


Figure 1: Timeline of the production simulation in one step.

We present the simulation algorithm of consumption in Algorithm 1 for process i . From line 2 to line 3, Algorithm 1 firstly computes the total number of consumption- ΔC_i in line 2 and then updates the state vector in line 3. Lines 4-7 create intermediate variables stored in the queue structure.

Algorithm 1 Consumption

- 1: Inputs: $t, \Delta t, \mathbf{x}, \hat{n}_i, N_q, \lambda_i^{max}, \{\alpha_{ij}\}, \hat{t}_i^{min}, \hat{t}_i^{max}$
 - 2: compute ΔC_i using (4)
 - 3: update $\{\hat{x}_{ij}\}$ using (5)
 - 4: $N_q \leftarrow N_q + 1$
 - 5: $d_{N_q} \leftarrow i$
 - 6: $Q_{N_q}^{delay} \leftarrow \Delta C_i$
 - 7: compute $t_{N_q}^s$ and $t_{N_q}^{span}$ using (6) and (7), respectively
-

2.2. Delayed production

Productions are expected as long as $N_q \geq 1$. The simulation algorithm then check if there is any scheduled production due to occur in the current time bucket, i.e., all the $n_q \in \{1, \dots, N_q\}$ which satisfy $t \leq t_{n_q}^s < t + \Delta t$. Assuming that the productions are uniformly distributed over time, the number of completed productions are proportional to the time fraction $t + \Delta t - t_{n_q}^s$ w.r.t. the total span $t_{n_q}^{span}$. Consequently, we update the associated components of the state vector- $\{\tilde{x}_{ik}\}, Q_{n_q}^{delay}, t_{n_q}^s$ and $t_{n_q}^{span}$ respectively. The details of the computations related to delayed production are summarized in Algorithm 2.

Algorithm 2 Production

```
1: Inputs:  $t, \Delta t, \{\tilde{n}_i\}, \mathbf{x}, \{\beta_{ik}\}, \{Q_{n_q}^{delay}\}, \{t_{n_q}^s\}, \{t_{n_q}^{span}\}, \{d_{n_q}\}$ 
2: for  $n_q \in \{1, \dots, N_q\}$  do
3:    $i \leftarrow d_{n_q}$ 
4:   if  $t_{n_q}^{span} > 0$  AND  $t_{n_q}^s < t + \Delta t$  then
5:      $\Delta P_i \leftarrow Q_{n_q}^{delay} \min(\frac{t + \Delta t - t_{n_q}^s}{t_{n_q}^{span}}, 1)$ 
6:      $\tilde{x}_{ik}(t) \leftarrow \tilde{x}_{ik}(t - \Delta t) + \beta_{ik} \Delta P_i, \quad k = 1 : \tilde{n}_i.$ 
7:      $Q_{n_q}^{delay} \leftarrow Q_{n_q}^{delay} - \Delta P_i$ 
8:      $t_{n_q}^s \leftarrow t + \Delta t$ 
9:      $t_{n_q}^{span} \leftarrow \max(0, t_{n_q}^{span} - (t + \Delta t - t_{n_q}^s))$ 
10:  end if
11: end for
```

2.3. Push system of supply chain

A supply chain push system [5] controls the production flow moving from the supply end to the final retailer end, with the purpose of firstly fulfilling the raw materials in the supply end, and then starting the procedure of production according to its prediction of demands.

Incorporating Algorithm 1 and Algorithm 2, we present Algorithm 3 which simulates a push system of supply chain. Note that we may need to adjust the length of the last time bucket to ensure the simulation stops at $t = T$ (lines 11-14 of Algorithm 3), where T is the end time of the simulation.

2.4. Pull system of supply chain

A pull system is a different design of supply chains compared with a push design in that its productions and inventories managements are driven by incoming orders [5]. In this section, we firstly describe the time bucket algorithms for inventory management and order projection before we introduce the full time bucket algorithm of pull system.

2.4.1. Inventory management

A safety stock is a popular and easy-to-implement remedy to mitigate disruptions in supply-chain operations [27] which can be caused by the temporal variations of product orders and the uncertainties in the supply. One strategy we can use to update the inventory is by adding the back order quantity when the inventory is less than the safety stock as follows

$$x_p^b(t) = \begin{cases} S_p & \text{if } x_p(t) \leq x_p^s \\ 0 & \text{otherwise} \end{cases}, \quad (8)$$

Algorithm 3 Push System of Supply Chain

```
1: Inputs:  $T, \Delta t, n, \{\tilde{n}_i\}, \{\hat{n}_i\}, \{\alpha_{ij}\}, \{\beta_{ik}\}, \{\lambda_i^{max}\}, \{\hat{t}_i^{min}\}, \{\hat{t}_i^{max}\}$  and  $\{\hat{x}_{ij}(0)\}$ 
2:  $N_q \leftarrow 0, t \leftarrow \min(\Delta t, T)$ 
3: while  $t \leq T$  do
4:    $x(t) = x(t - \Delta t)$ 
5:   for all  $i \in \{1, \dots, n\}$  do
6:     goto Algorithm 1
7:   end for
8:   if  $N_q \geq 1$  then
9:     goto Algorithm 2
10:  end if
11:  if  $t + \Delta t > T$  then
12:     $\Delta t \leftarrow T - t$ 
13:  end if
14:   $t \leftarrow t + \Delta t$ 
15: end while
```

where $p \in \mathbb{S}$ is a raw material, x_p^s is the safety stock, S_p is a constant used as a safeguard for the stock of part p . Another possible way to place the back order can be

$$x_p^b(t) = \begin{cases} x_p^s - x_p(t) + S_p & \text{if } x_p(t) \leq x_p^s \\ 0 & \text{otherwise} \end{cases},$$

which is more resilient towards uncertainties in the supply chain network. On the other hand, when we increase the amount of inventory, we expect increased storage costs. Finding a good balance between the safety stock x_p^s , safeguard S_p , order delay t_p^d and costs, remains challenging in practice. The optimal strategy for inventory management is problem specific, and an extensive literature has been devoted to this topic [15, 33, 9, 27].

Let \bar{t}_p denote the time when the next supply of part p arrives. Given a constant $M > T$, our inventory management can be summarized as in Algorithm 4 for each time t when we update the system state.

2.4.2. Projected order and pull system

Once a demand order is given, a supply chain system firstly check if sufficient inventory exists to meet the demand. If there is not enough inventory to fulfill the demand, the supply chain needs to start the procedure of production in order to match the gap. We then need to perform a back track to see if the existing inventories of all the intermediate parts, on the path of the flow chart, can satisfy their own demands.

Algorithm 4 Inventory Management

```

1: Inputs:  $t, \mathbf{x}, \{t_p^d\}, \{\bar{t}_p\}, M, \{x_p^s\}, \{S_p\}$ 
2: for all  $p \in \mathbb{S}$  do
3:   compute  $x_p^b$  using (8)
4:   if  $t \geq \bar{t}_p$  then
5:      $x_p \leftarrow x_p + x_p^b$ 
6:      $\bar{t}_p \leftarrow M$ 
7:   else if  $t < \bar{t}_p$  AND  $\bar{t}_p = M$  AND  $x_p^b > 0$  then
8:      $\bar{t}_p \leftarrow t + t_p^d$ 
9:   end if
10: end for

```

To guarantee that all the demands are satisfied, the projected accumulated demand g_p , which includes the number of parts that is consumed in the intermediate processes, should be calculated by the following recursive function

$$g_p(t) = \begin{cases} \hat{g}_p(t) & \text{if } p \in \mathbb{E} \\ \sum_{\{(i,j)|\hat{p}_{ij}=p\}} \alpha_{ij} \max_k \left(\left\lceil \frac{g_{\hat{p}_{ik}}}{\beta_{ik}} \right\rceil \right) + \hat{g}_p(t) & \text{otherwise} \end{cases}, \quad (9)$$

where $\hat{g}_p = \sum_{\tau \leq t} g_p^*(\tau)$ is the total order of part $p \in \mathbb{P}$ accumulative in time up to t , where $\{\tau\}$ are discrete time points in the simulation, $g_p^*(\tau)$ is the incoming order of part $p \in \mathbb{P}$ at time τ , $\lceil x \rceil = \min\{m \in \mathbb{Z} | m \geq x\}$ is the ceiling function. This step can be visualized by a process starting from the final product. For example, we have a small supply chain which has four parts involved as shown in Figure 2. One part A makes one part B, and one part D is assembled from one part B and one part C. Assuming we have some spare part orders at time t on part B and D, and each order requires 100 units of the corresponding part. By the backward recursion (9), we can compute the projected demand for each part as 200, 200, 100 and 100, respectively.

The projected value g_p indicates the necessary quantity of part p that needs to be produced to satisfy the given orders. Quantity $g_p - \hat{g}_p$ then represents the least number that part p still need to be consumed during the following consumption-production processes. Due to the size of time bucket, the real consumption may be larger than $g_p - \hat{g}_p$. Therefore, by comparing the accumulated consumption $c_p(t) = \sum_{\tau \leq t} \sum_{\{(i,j)|\hat{p}_{ij}=p\}} \alpha_{ij} \Delta C_i(\tau)$ with $g_p - \hat{g}_p$, we can understand whether or not part p should be further consumed. In the above example, we assume 50 Part B has been consumed in the simulation. Since $50 = c_p < g_p - \hat{g}_p = 200 - 100 = 100$, it indicates Part B still needs to be consumed to build Part D. Similarly, if $c_p \geq g_p - \hat{g}_p$, it implies that part p has already been consumed sufficiently, and no more consumption should happen to it. The projected order and pull strategy is summarized in Algorithm 5,

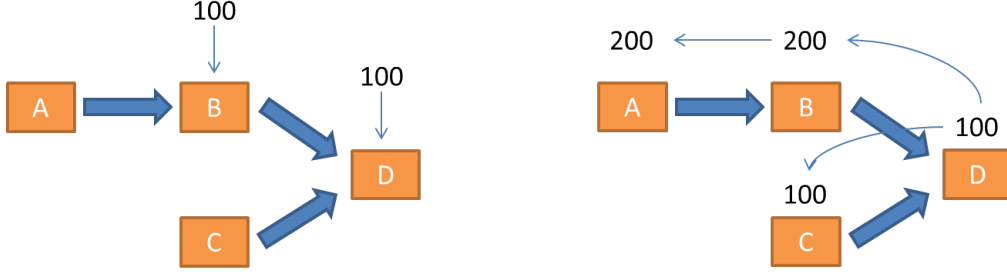


Figure 2: Left picture shows that there are two orders on part B and D, and each order requires an amount of 100 units. Right picture shows the projected demand of each part.

where variable $flag$ is introduced for each process in order to control the consumption.

Algorithm 5 Projected Order and Pull Strategy

```

1: Inputs:  $n, \{\hat{g}_p\}, \{c_p\}, \{\alpha_{ij}\}, \{\beta_{ik}\}$ 
2: for all  $i \in \{1, \dots, n\}$  do
3:    $flag_i \leftarrow 0$ 
4: end for
5: for all  $p \in \mathbb{P}$  do
6:   compute  $g_p$  using (9)
7:   if  $c_p < g_p - \hat{g}_p$  then
8:     for all  $i \in \{i \mid \exists \hat{p}_{ij} = p\}$  do
9:        $flag_i \leftarrow 1$ 
10:    end for
11:  end if
12: end for

```

Remark 1. *The simulation using the proposed algorithms (Algorithm 3 and Algorithm 6), approaches the results from DES, when the time interval Δt is small enough.*

3. Stochastic time bucket method: L-leap

In the previous sections we presented the deterministic time bucket approximation of DES, where the number of processes happening during a fixed time interval is a deterministic value, i.e., $\Delta C_i = \lambda_i(t)\Delta t$, $i = 1, \dots, n$. A more realistic simulation should consider random noises in the processes. By introducing randomnesses into the simulation, it also allows us to have a better understanding about the potential risk in the supply-chain system. Similar to D-leap [3], we treat both consumption ΔC_i and delayed production ΔP_i as random variables.

Algorithm 6 Time Bucket Simulation of Supply Chain-Pull System

```

1: Inputs:  $T, \Delta t, n, \{\tilde{n}_i\}, \{\hat{n}_i\}, \{\alpha_{ij}\}, \{\beta_{ik}\}, \{\lambda_i^{max}\}, \{\hat{t}_i^{min}\}, \{\hat{t}_i^{max}\}, \{\hat{x}_{ij}(0)\}, \{t_p^d\}, \{\bar{t}_p\}, M, \{x_p^s\}, \{S_p\},$ 
    $\{\hat{g}_p\}$ 
2:  $N_q \leftarrow 0, t \leftarrow \Delta t, \{\bar{t}_p\} \leftarrow M, \{c_p\} \leftarrow 0$ 
3: while  $t \leq T$  do
4:    $x(t) = x(t - \Delta t)$ 
5:   goto Algorithm 4
6:   goto Algorithm 5
7:   for all  $i \in \{1, \dots, n\}$  do
8:     if  $flag_i > 0$  then
9:       goto Algorithm 1
10:    for all  $j \in \{1, \dots, \hat{n}_i\}$  do
11:       $c_{\hat{p}_{ij}} \leftarrow c_{\hat{p}_{ij}} + \alpha_{ij} \Delta C_i$ 
12:    end for
13:  end if
14: end for
15: if  $N_q \geq 1$  then
16:   goto Algorithm 2
17: end if
18: if  $t + \Delta t \geq T$  then
19:    $\Delta t \leftarrow T - t$ 
20: end if
21:  $t \leftarrow t + \Delta t$ 
22: end while

```

The number of processes happening in Δt follows a Poisson distribution with parameter $\lambda_i \Delta t$:

$$\Delta C_i \sim Poi(\lambda_i \Delta t), \quad i = 1, \dots, n \quad (10)$$

and the number of productions follows a binomial distribution:

$$\Delta P_{d_{n_q}} \sim B(Q_{n_q}^{delay}, \min(\frac{t + \Delta t - t_{n_q}^s}{t_{n_q}^{span}}, 1)) \quad n_q = 1, \dots, N_q. \quad (11)$$

The stochastic simulation procedures for consumption and production are presented in Algorithms 7 and 8, respectively. The stochastic consumption and production can be easily embedded in the simulation flow of Algorithm 6 which lead to a new stochastic simulation strategy implemented using Algorithm 9. We call it the L(logistic)-leap method, where we use a constant average production rate and boolean values associated

with the inventory policies and the order projections at time t to predict the productions during t and $t + \Delta t$. Note that the approximation is used such that we have the flexibility to accelerate the computation under prescribed numerical tolerance. Indeed, we will show that uncertainty propagation in supply chains can be dramatically accelerated without sacrificing any accuracy if we use the time bucket simulation in a coordinated way.

Algorithm 7 Consumption with Uncertainties

- 1: Inputs: $t, \Delta t, \mathbf{x}, \{\hat{n}_i\}, n_q, \{\lambda_i^{max}\}, \{\alpha_{ij}\}, \{\hat{t}_i^{min}\}, \{\hat{t}_i^{max}\}$
 - 2: compute ΔC_i using (10)
 - 3: update $\{\hat{x}_{ij}\}$ using (5)
 - 4: $d_{n_q} \leftarrow i$
 - 5: $Q_{n_q}^{delay} \leftarrow \Delta C_i$
 - 6: compute $t_{n_q}^s$ and $t_{n_q}^{span}$ using (6) and (7), respectively
 - 7: $n_q \leftarrow n_q + 1$
-

Algorithm 8 Production with Uncertainties

- 1: Inputs: $t, \Delta t, \mathbf{x}, \{\tilde{n}_i\}, N_q, \{\beta_{ik}\}, \{Q_{n_q}^{delay}\}, \{t_{n_q}^s\}, \{t_{n_q}^{span}\}, \{d_{n_q}\}$
 - 2: **for** $n_q \in \{1, \dots, N_q\}$ **do**
 - 3: $i \leftarrow d_{n_q}$
 - 4: **if** $t_{n_q}^{span} > 0$ **AND** $(t_{n_q}^s < t + \Delta t)$ **then**
 - 5: compute ΔP_i using (11)
 - 6: $\tilde{x}_{ik}(t) \leftarrow \tilde{x}_{ik}(t - \Delta t) + \beta_{ik} \Delta P_i(t), \quad k = 1 : \tilde{n}_i.$
 - 7: $Q_{n_q}^{delay} \leftarrow Q_{n_q}^{delay} - \Delta P_i$
 - 8: $t_{n_q}^s \leftarrow t + \Delta t$
 - 9: $t_{n_q}^{span} \leftarrow \max(0, t_{n_q}^{span} - (t + \Delta t - t_{n_q}^s))$
 - 10: **end if**
 - 11: **end for**
-

4. Uncertainty propagation using time bucket simulation and MLMC

In this section, we describe the problem of uncertainty forward propagation, the MC discretization of an expectation, and the MLMC approach to compute the expectation. MLMC was combined with Tau-leap for uncertainty quantification in the context of stochastic chemical reactions in [1, 25].

Forward uncertainty propagation is concerned about the estimation of the expected value of a quantity of interest(q), e.g., q can be the delivery time of the final products. The standard MC estimator reads

Algorithm 9 L-leap Simulation of Supply Chains with Uncertainties - Pull System

```

1: Inputs:  $T, \Delta t, n, \{\tilde{n}_i\}, \{\hat{n}_i\}, \{\alpha_{ij}\}, \{\beta_{ik}\}, \{\lambda_i^{max}\}, \{\hat{t}_i^{min}\}, \{\hat{t}_i^{max}\}, \{\hat{x}_{ij}(0)\}, \{t_p^d\}, \{\bar{t}_p\}, M, \{x_p^s\}, S_p, \{\hat{g}_p\}$ 
2:  $N_q \leftarrow 0, t \leftarrow \Delta t, \{\bar{t}_p\} \leftarrow M, \{c_p\} \leftarrow 0$ 
3: while  $t \leq T$  do
4:    $x(t) = x(t - \Delta t)$ 
5:   goto Algorithm 4
6:   goto Algorithm 5
7:   for all  $i \in \{1, \dots, n\}$  do
8:     if  $flag_i > 0$  then
9:       goto Algorithm 7
10:    for all  $j \in \{1, \dots, \hat{n}_i\}$  do
11:       $c_{\hat{p}_{ij}} \leftarrow c_{\hat{p}_{ij}} + \alpha_{ij} \Delta C_i$ 
12:    end for
13:  end if
14: end for
15: if  $N_q \geq 1$  then
16:   goto Algorithm 8
17: end if
18: if  $t + \Delta t \geq T$  then
19:    $\Delta t \leftarrow T - t$ 
20: end if
21:  $t \leftarrow t + \Delta t$ 
22: end while

```

$$\mathbf{E}_{\boldsymbol{\theta}, \omega} [q(\boldsymbol{\theta}, \omega)] = \frac{1}{N_s} \sum_{k=1}^{N_s} q(\boldsymbol{\theta}_k, \omega_k) + \mathcal{O}_{\mathcal{P}} \left(\frac{1}{\sqrt{N_s}} \right), \quad (12)$$

where $\boldsymbol{\theta}$ is the vector of random parameters, ω is the noise which perturbs the system states dynamically, N_s is the number of samples. The notation of sequence of random variables $Y_{N_s} = \mathcal{O}_{\mathcal{P}}(d_{N_s})$ indexed by N_s means that for any $\epsilon > 0$, there exists a finite K and a finite N_0 , such that for any $N_s > N_0$, the probability $Pr(Y_{N_s} > K d_{N_s})$ is smaller than ϵ . Assigning a tolerance ϵ_s and a confidence level α on the statistical error leads to

$$Pr \left(\left| \frac{1}{N_s} \sum_{k=1}^{N_s} q(\boldsymbol{\theta}_k, \omega_k) - \mathbf{E}_{\boldsymbol{\theta}, \omega} [q(\boldsymbol{\theta}, \omega)] \right| < \epsilon_s \right) = \alpha \quad (13)$$

Based on the Central Limit Theorem (CLT), the computational cost of a standard MC sampler which satisfies the above error bound with probability $\alpha \rightarrow 1$ is as follows :

$$C_{mc} = C_m V \Phi^{-2}\left(\frac{1+\alpha}{2}\right) \epsilon_s^{-2}, \quad (14)$$

where C_{mc} is the total cost, V is the variance of the quantity of interest, C_m is the average cost of a single DES, $\Phi^{-1}(\cdot)$ is the inverse distribution function of the standard normal distribution, ϵ_s is the tolerance on the absolute error committed by the MC estimator.

MLMC approach is a powerful sampling method to accelerate the computation of an expectation via drawing samples from a hierarchy of models. It is optimized in the sense that the total computational cost is minimized for a given tolerance on the numerical error. In the hierarchy of models, high level models are more accurate and computationally more expensive than low level models. Provided that the expectation and variance of the difference between the approximated and the true solutions diminish at certain rates, as the level increases, we can construct an MLMC sampler, which can be several orders more efficient than the standard MC method. Note that standard MC method would put all its samples on the highest level to control the bias of the estimator. Let q_l denote the corresponding level l approximation of the quantity of interest q . Assume that the numerical discretization error is bounded uniformly in the probability space as follows

$$\mathbf{E}(q - q_l) = \mathcal{O}(\Delta t_l^a), \quad (15)$$

where Δt_l is the size of the time bucket on level l , $a \in \mathbb{R}^+$ is the convergence rate of the numerical discretization, the notation $Y_{\Delta t} = \mathcal{O}(d_{\Delta t})$ indexed by Δt is the deterministic version of $Y_{\Delta t} = \mathcal{O}_{\mathcal{P}}(d_{\Delta t})$, which means that there exists a finite K and a finite Δt_0 , such that for any $\Delta t < \Delta t_0$, $Y_{\Delta t} \leq K d_{\Delta t}$.

The expectation in (12) can be rewritten as a telescopic sum as follows

$$\mathbf{E}(q) = \sum_{l=0}^L \mathbf{E}(q_l - q_{l-1}) + \mathcal{O}(\Delta t_L^a), \quad \text{with } q_{-1} = 0. \quad (16)$$

Furthermore, we can write the first term on the right hand side (r.h.s.) of Equation (16) as a summation of sample averages, and (16) becomes

$$\mathbf{E}(q) = \hat{q} + \sum_{l=0}^L \mathcal{O}_{\mathcal{P}}\left(\frac{1}{\sqrt{N_l}}\right) + \mathcal{O}(\Delta t_L^a), \quad \text{with } q_{-1} = 0, \quad (17)$$

where

$$\hat{q} = \sum_{l=0}^L \frac{1}{N_l} \sum_{k=1}^{N_l} (q_l^k - q_{l-1}^k), \quad (18)$$

is the MLMC estimator of q , $\sum_{l=0}^L \mathcal{O}_{\mathcal{P}}\left(\frac{1}{\sqrt{N_l}}\right)$ is the statistical error, $\mathcal{O}(\Delta t_L^a)$ is the numerical bias. A heuristic argument on the computational advantage of using this estimator is the following: the variance of $q_l - q_{l-1}$ becomes very small as l increases, hence we draw few high-level samples while most of the samples are shifted to the lower levels where the computations are fast.

Next, we optimize the computational cost of the MLMC estimator for given tolerances on the bias and the statistical error which read

$$\mathbf{E}(q - q_L) = \epsilon_b, \quad (19)$$

$$\Pr(|\hat{q} - \mathbf{E}(q_L)| < \epsilon_s) = \alpha, \quad (20)$$

where ϵ_b is the tolerance on the bias, ϵ_s is the tolerance on the statistical error. Note that we can use CLT to convert (20) to the following variance constraint:

$$\mathbf{Var}(\hat{q}) = \frac{\epsilon_s^2}{\Phi^{-2}\left(\frac{1+\alpha}{2}\right)}. \quad (21)$$

The maximum level can be obtained from (15) and (19):

$$L = \frac{1}{a} \log_2(\epsilon_b),$$

assuming that $2^{-l} = \Delta t_l$.

The optimal number of samples on each level can be obtained by minimizing the total cost under the constraint (21) on the variance of the estimator:

$$\{N_l^{opt}, l = 0, \dots, L\} = \arg \min_{\{N_l, l=0, \dots, L\}} \left[\sum_{l=0}^L C_l N_l + \lambda \left(\sum_{l=0}^L \frac{V_l}{N_l} - \frac{\epsilon_s^2}{\Phi^{-2}\left(\frac{1+\alpha}{2}\right)} \right) \right],$$

where C_l is the average computational cost of $q_l - q_{l-1}$, V_l is the variance of the random variable $q_l - q_{l-1}$, λ is a Lagrangian multiplier (by an abuse of notation).

Solving the above minimization problem leads to

$$N_l^{opt} = \sqrt{\frac{V_l}{C_l} \frac{\sum_{l=0}^L \sqrt{C_l V_l}}{\bar{\epsilon}_s^2}} \quad \text{with} \quad \bar{\epsilon}_s^2 = \frac{\epsilon_s^2}{\Phi^{-2}\left(\frac{1+\alpha}{2}\right)}.$$

Consequently, the optimal total computational cost of the multilevel estimator is

$$\begin{aligned} \sum_{l=0}^L C_l N_l^{opt} &= \sum_{l=0}^L C_l \sqrt{\frac{V_l}{C_l} \frac{\sum_{l=0}^L \sqrt{C_l V_l}}{\bar{\epsilon}_s^2}} \\ &= \left(\sum_{l=0}^L \sqrt{C_l V_l} \right)^2 \bar{\epsilon}_s^{-2}. \end{aligned}$$

It is common that the variance V_l and cost C_l have the asymptotic bounds: $V_l = \mathcal{O}(\Delta t_l^b)$ and $C_l = \mathcal{O}(\Delta t_l^{-g})$, where b and g are the rates which describe the algebraic decrease/grow of the variances and

computational costs, respectively. In the cases where $C_0V_0 \gg C_1V_1 \gg \dots \gg C_LV_L$, the total cost is dominated by $C_0V_0\bar{\epsilon}_s^{-2}$. In the cases where $C_LV_L \gg C_{L-1}V_{L-1} \gg \dots \gg C_0V_0$, the total cost is dominated by $C_LV_L\bar{\epsilon}_s^{-2} = C_0V_0\epsilon_b^{-\frac{g-b}{a}}\bar{\epsilon}_s^{-2}$. In the cases where $C_LV_L = C_{L-1}V_{L-1} = \dots = C_0V_0$, the total cost is $L^2C_0V_0\bar{\epsilon}_s^{-2} = C_0V_0(\log_2\epsilon_b)^2\bar{\epsilon}_s^{-2}/a^2$. Note that in the literature, it is common to impose a total tolerance ϵ^2 on the mean square error of the MLMC estimator and split the error budget into two parts - $\theta\epsilon^2$ and $(1-\theta)\epsilon^2$ ($0 < \theta < 1$) on the bias and variance [22, 12, 13]. We give an explicit confidence level to the statistical error control in this study which is consistent to the literature such as [8, 25, 4].

Remark 2. *The complexity of a standard MC sampler is $\mathcal{O}\left(\bar{\epsilon}_s^{-2}\epsilon_b^{-\frac{g}{a}}\right)$, where $\bar{\epsilon}_s^{-2}$ is the complexity of a standard MC, $\epsilon_b^{-\frac{g}{a}}$ is associated with the computational cost of each sample on level L . In our study, the average cost of an exact DES is similar to the average cost of its time bucket approximation on the highest level, i.e., $C_L \approx C_m$. Therefore, the computational complexity of MC (14) would always be higher than that of the MLMC asymptotically.*

Remark 3. *The q_l^k and q_{l-1}^k in (18) should always be computed using the same realization of the random parameters as their inputs, to assure the correlation between q_l and q_{l-1} . In the cases where the randomness is driven by stochastic processes, we adopt the coupling scheme proposed as the Algorithm 2 in [1]. The key idea of this algorithm was to use the additivity property of Poisson processes to tightly correlate two processes on different levels.*

5. Numerical example

We present in this section five numerical examples with increasing complexities. The first example is a push system simulated using deterministic and stochastic time bucket methods. The second example is a pull system, in which the material flow is driven by the orders from the downstream customers. The third example is a pull system considering back-ordering, priority delivery, and transportation delays simulated using time bucket methods. We finally carry out uncertainty propagation using MLMC in the fourth and fifth examples.

5.1. Time bucket approximations of a simple push supply chain network

We consider a supply chain system for manufacturing industry which is schematically shown in Figure 3. It involves five processes and eight parts, and we show the consumption-production relationships in equations (22)-(26). The parts on the left hand side of the equations are instantaneously consumed when the processes get started, while the parts on the r.h.s. are produced after certain periods of delays, characterized by the production time/lead time of each process. The production rate which describes the capacity of a process is the number of parts which get processed in a time unit, e.g., one day.

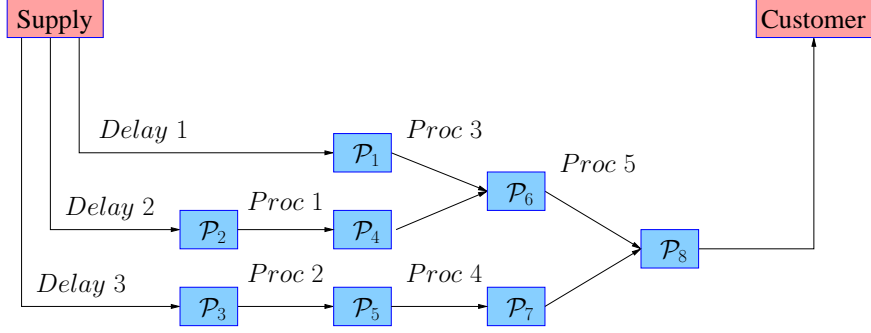


Figure 3: A manufacturing system with five processes and eight parts.

$$\mathcal{P}_2 = \mathcal{P}_4 \quad (22)$$

$$\mathcal{P}_3 = \mathcal{P}_5 \quad (23)$$

$$\mathcal{P}_1 + \mathcal{P}_4 = \mathcal{P}_6 \quad (24)$$

$$\mathcal{P}_5 = \mathcal{P}_7 \quad (25)$$

$$\mathcal{P}_6 + \mathcal{P}_7 = \mathcal{P}_8 \quad (26)$$

A push system starts the procedure of production according to its prediction of demands. We assume the following initial conditions: $x_1(t=0) = 1000$, $x_2(t=0) = 500$, $x_3(t=0) = 1000$, which prescribe the initial inventory levels of \mathcal{P}_1 , \mathcal{P}_2 and \mathcal{P}_3 . For all $i \notin \mathbb{S}$, i.e., the intermediate and final products, we let $x_i(t=0) = 0$. Firstly we assume deterministic production rates which read $\lambda_1 = 8$, $\lambda_2 = 8$, $\lambda_3 = 4$, $\lambda_4 = 8$ and $\lambda_5 = 2$. We also assume the processing time is deterministic, i.e., $\hat{t}_i^{max} = \hat{t}_i^{min}$, $i = 1, \dots, 5$, and they are specifically $\hat{t}_1^{min} = 1$, $\hat{t}_2^{min} = 1$, $\hat{t}_3^{min} = 10$, $\hat{t}_4^{min} = 1$, $\hat{t}_5^{min} = 10$.

Figure 4 shows the time histories of the state vector, which represents the number of each part in the system at any given time, simulated under two different values of the time bucket. Note that the time bucket approximation is able to capture the main dynamical features of the system even when a coarse time bucket size, $\Delta t = 16$ days, is used. The monotonic decrease of \mathcal{P}_1 stopped at 500 due to the initial inventory level of \mathcal{P}_2 . x_8 monotonically increases after an initial period of waiting which attributes to the production delays. The dynamics of the intermediate parts - \mathcal{P}_4 , \mathcal{P}_5 , \mathcal{P}_6 and \mathcal{P}_7 are majorly determined by their consumption and production rates.

It is shown in Figure 5 that the time bucket method converges to the “ground truth” computed by DES, when Δt reduces from 32 days to 4 days. The error is smaller than 2% when the time bucket is smaller than 4 days.

The absolute error of the 200 days’ production decreases linearly when time bucket size decreases as shown in the left picture of Figure 6. The CPU time of the time bucket approximation increases linearly as

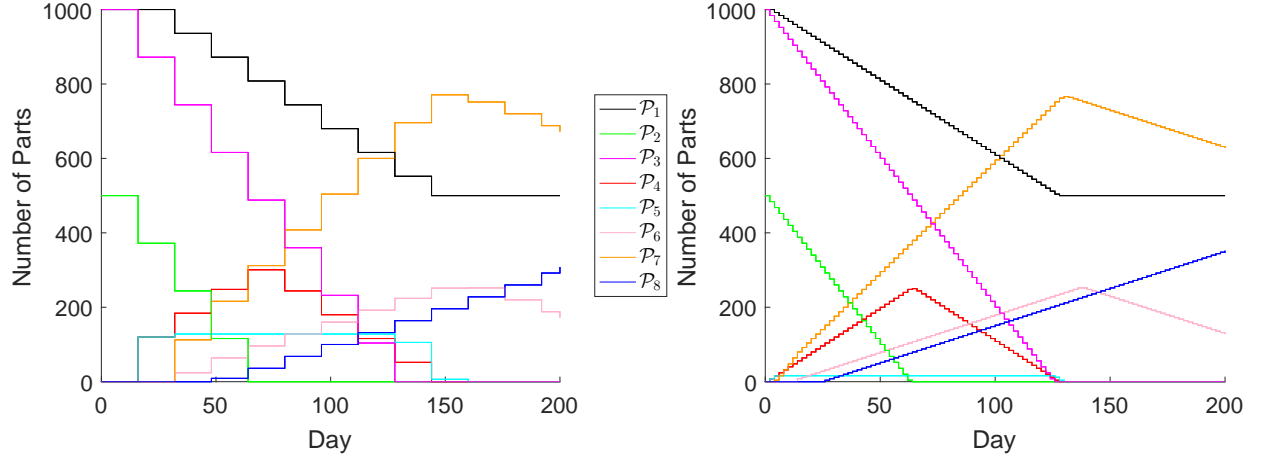


Figure 4: The time history of the state vector in push system. From left to right, figures present the case for $\Delta t = 16$ days and $\Delta t = 2$ days, respectively.

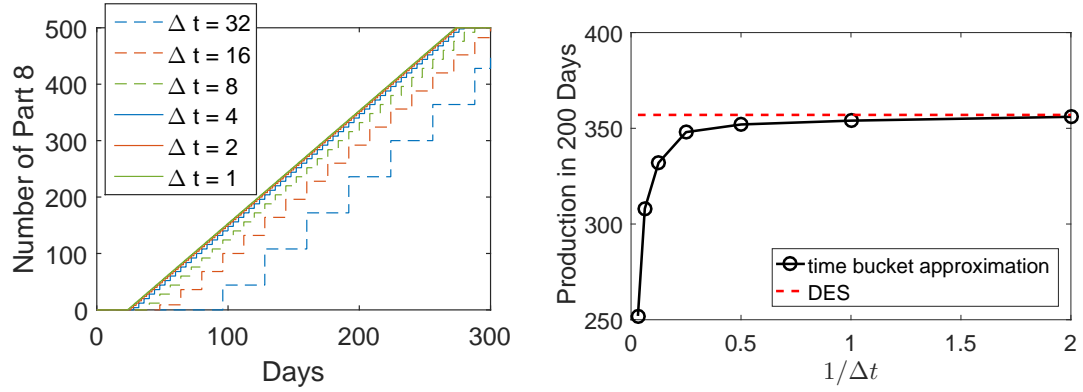


Figure 5: Push system. Left figure is the simulated evolution of the number of final products (\mathcal{P}_8); right figure is the convergence of the number of product in 200 days w.r.t. the reciprocal of the size of time bucket. The reference value is 357.

we increase the number of time buckets during the simulation time (The CPU time is an average value over 100 repetitive runs).

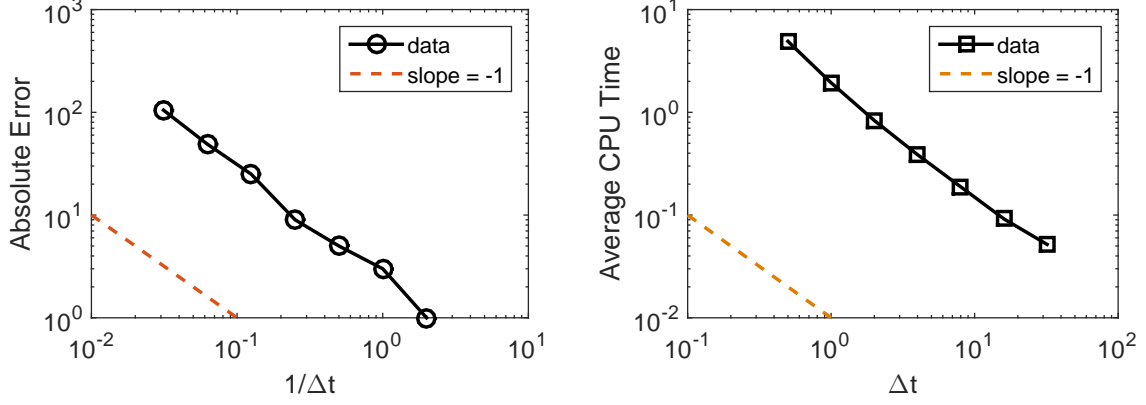


Figure 6: Push system. Left figure is the absolute error of the 200 days production w.r.t. the reciprocal of the size of time bucket. Right figure is the CPU time averaged over 100 repetitive runs of the simulation up to 200 days, w.r.t. the size of time bucket.

Next, we use the L-leap method to approximately simulate the stochastic system where the state vector is dynamically driven by Poisson processes. Figure 7 visualizes 1000 trajectories using identical initial data. It is noteworthy that uncertainties accumulate in time for this push system in that the variability of a trajectory becomes larger than that at a previous temporal coordinate.

In addition, we notice that the average trajectories shift from left to right when we reduce Δt , for example, the 500th \mathcal{P}_8 is produced in around 300 days when $\Delta t = 16$ days, while it is produced in around 270 days with $\Delta t = 2$ days. This is due to the artificially delayed availability of its previous parts when the time bucket is coarse.

5.2. Time bucket approximations of a supply network driven by downstream orders

We consider a pull system which starts to produce as soon as an order is received. The system receives 100 orders of the final product every 200 days, and the initial inventories of \mathcal{P}_1 , \mathcal{P}_2 and \mathcal{P}_3 are 1000 each. Figure 8 shows the trajectories of the numbers of parts in the system for 1000 days, where we can find that the trajectories of \mathcal{P}_2 and \mathcal{P}_3 are identical.

Furthermore, we show in Figure 9 the absolute consecutive error of the components of the state vector $\mathbf{x}_{\Delta t}(t = 200)$ using different Δt 's. We also observe that errors diminish at the rate of -1 (linearly) until the Δt is small enough to resolve every single event.

In a stochastic setting where the production is perturbed by a Poisson process, we use L-leap method to approximate the pull system. We again decrease the initial inventory of \mathcal{P}_2 from 1000 to 500, in order to distinguish its trajectory from \mathcal{P}_3 and observe how the other parts are affected in the simulation.

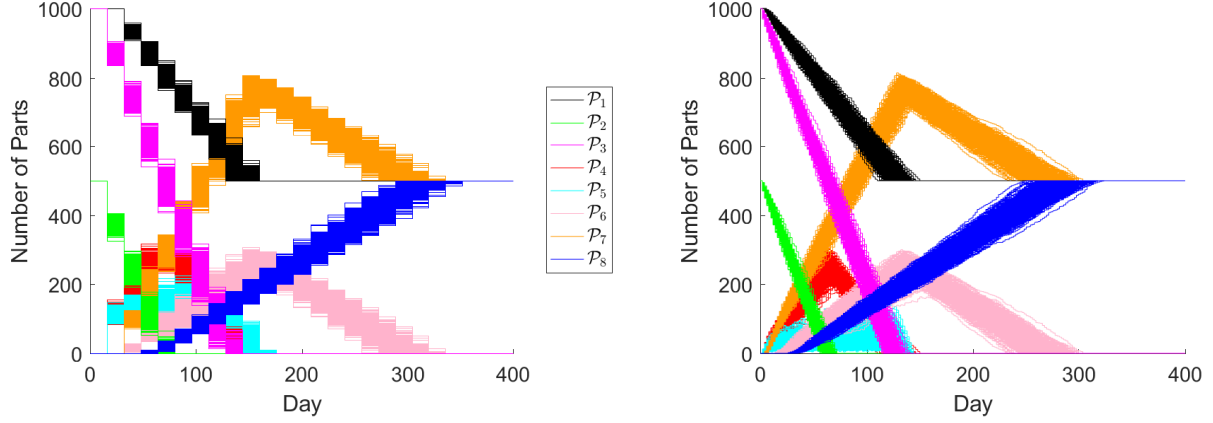


Figure 7: The time history of the state vector in stochastic push system. From left to right, figures present the case for $\Delta t = 16$ days and $\Delta t = 2$ days, respectively.

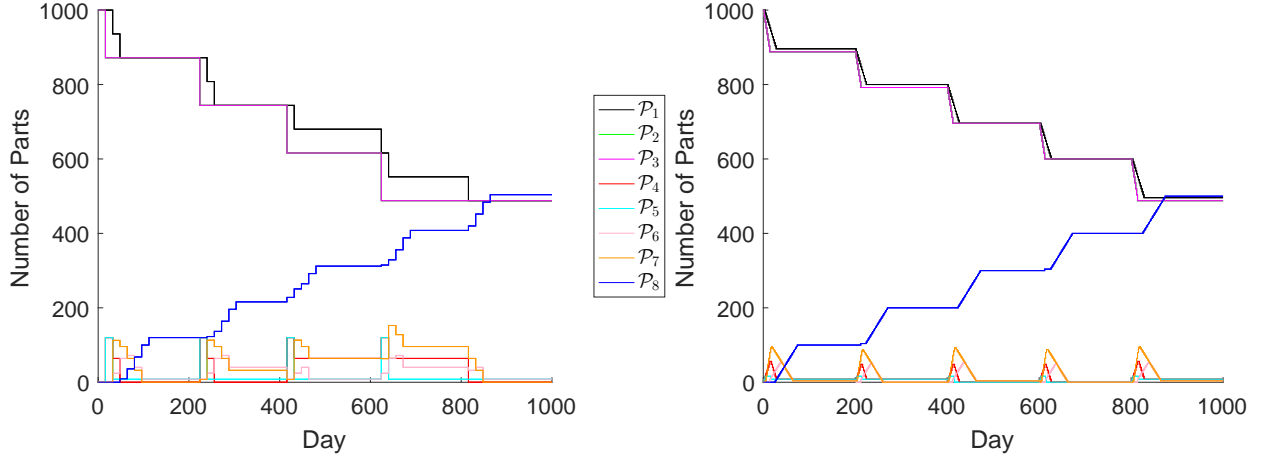


Figure 8: The time history of the state vector in pull system. From left to right, each picture presents a case for $\Delta t = 16$ days and $\Delta t = 2$ days, respectively.

The accumulation of uncertainties as observed in the push system is not presented in the pull system (see Figure 10) in that all the orders can be completed in the current cycle of production before the next order arrives. As a result, the simulation for each order seems independent to the previous ones, and therefore the average trajectory for each cycle looks identical to each other in Figure 10. This observation can also be obtained from Figure 11, which presents the mean value in black and the 95% confidence interval in red, for the material flows of \mathcal{P}_2 , \mathcal{P}_4 , \mathcal{P}_6 and \mathcal{P}_8 . The left pictures in Figure 11 show the sample statistics of 1000 random trajectories with $\Delta t = 16$ days, while the right pictures show the the sample statistics with $\Delta t = 2$ days. From Figure 11, it is clear that the standard deviation for each part accumulates dynamically when Δt is large. The standard deviation moderately increases until \mathcal{P}_2 runs out of stock towards the end of the simulations. Linear convergences are observed in Figure 12 where we plot the absolute consecutive error of

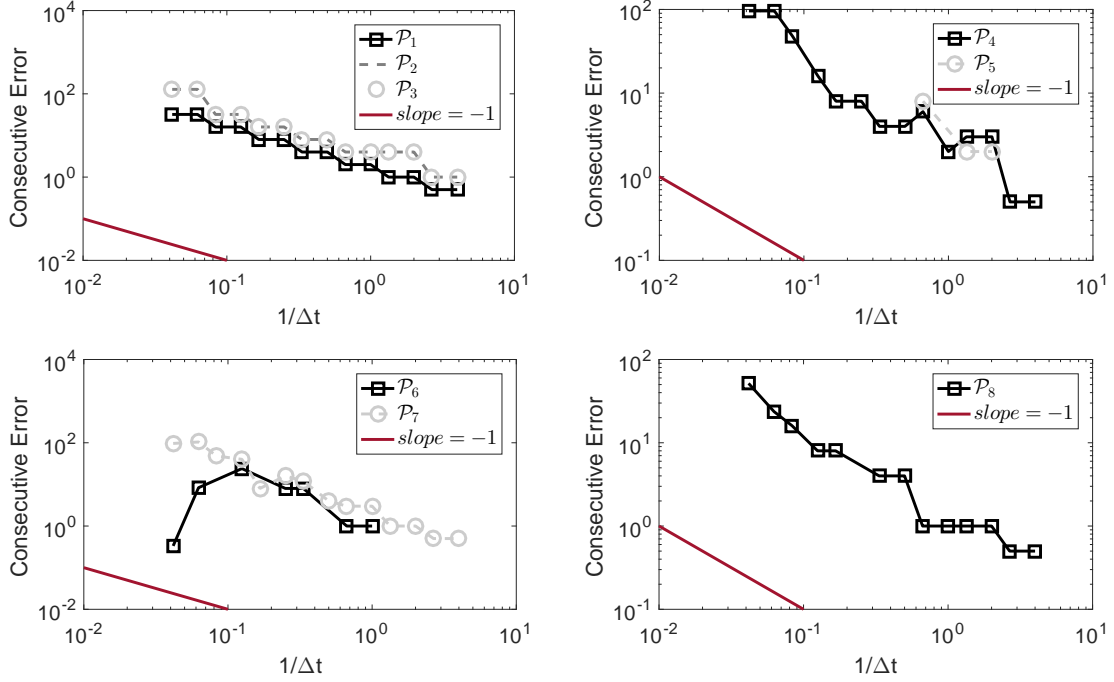


Figure 9: Pull system. The absolute consecutive errors of the numbers of the parts on the 200th day w.r.t. the time discretization.

the mean value of the number of parts on the 200th day, w.r.t. the size of time bucket.

5.3. Time bucket approximations of a complex pull system

This example is a pull system dealing with mixed orders of spare parts and final products, and considering transportation. The system receives spare-part orders of \mathcal{P}_4 , \mathcal{P}_5 , \mathcal{P}_6 and \mathcal{P}_7 every 50 days. Meanwhile, the following inventory policy is adopted to refill \mathcal{P}_1 , \mathcal{P}_2 and \mathcal{P}_3 : when the number of an inventory falls below 200, back orders of 200, 250 and 300 are placed for \mathcal{P}_1 , \mathcal{P}_2 and \mathcal{P}_3 , respectively. The delivery delays are 15, 20 and 30 days for \mathcal{P}_1 , \mathcal{P}_2 and \mathcal{P}_3 , respectively. Moreover, each of them has an initial inventory of 500. On top of the spare-part orders, we place three orders of final products on the first day, the 100th day and the 200th day, while each order consists 100 final products \mathcal{P}_8 . Upon the receipt of orders of the final products, the parts are used with priority for the production of the final products.

Additionally, transportation occurs between any two consecutive processes. The transportation of products are modeled as additional processes characterized by transportation rates and transportation delay time (similar to the production rates and the processing time of a production process). After renumbering and augmenting the original set of processes, the new system is shown in Figure 13, where the first five processes are the original processes; the second set of five processes are the transportation processes. For Processes 6-10, we use transportation rates $\lambda_i = 8, \forall i \in \{6, \dots, 10\}$ and constant transportation delay time

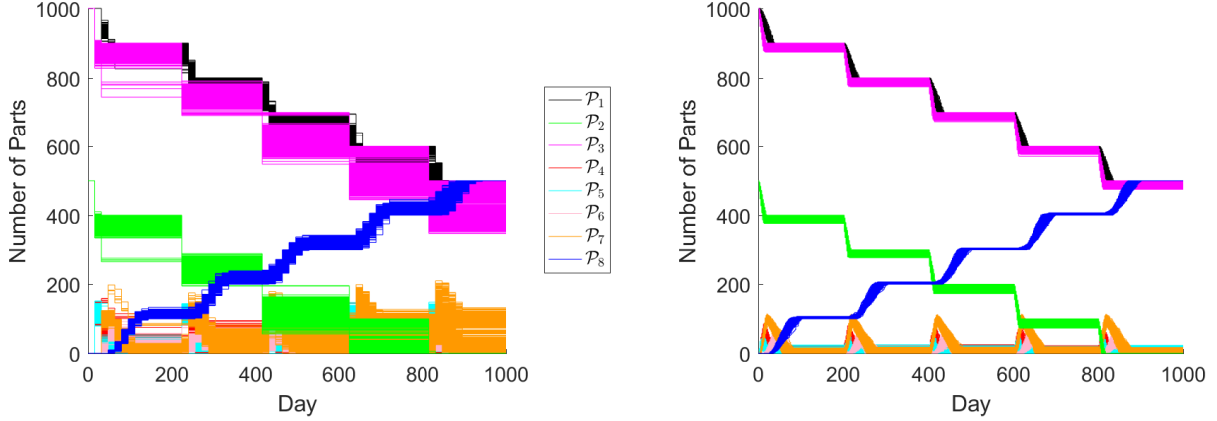


Figure 10: The time history of the state vector in stochastic pull system. From left to right, each picture presents a case for $\Delta t = 16$ days and $\Delta t = 2$ days, respectively.

$\hat{t}_i^{min} = \hat{t}_i^{max}$ are 10, 10, 10, 50 and 10 days, respectively.

Figure 14 shows the simulated numbers of parts in the system as they evolve in time using two different lengths of time buckets, i.e., $\Delta t = 16$ and 2 days. The start of the delivery of the final product- \mathcal{P}_{13} has been shifted to a later date compared to that of the case without transportation. Thanks to the creation of the new processes, we are able to simulate the number of goods in the buffers after their delayed production, during the transportation and in the buffers before their instantaneous consumption.

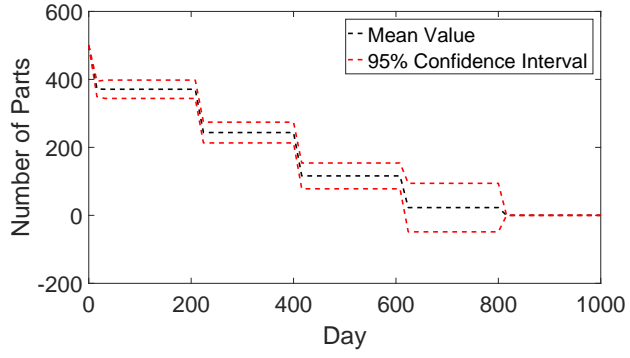
Additionally, we simulate a stochastic pull system with mixed orders and transportation using the L-leap method. We present the average number and its 95% confidence interval in 700 days for part \mathcal{P}_1 , \mathcal{P}_2 , \mathcal{P}_3 and \mathcal{P}_{13} , i.e., the raw materials and the final product, in Figure 15. It is noteworthy that very large uncertainties exists at the points where inventories possibly get refilled.

5.4. Uncertainty propagation using MLMC - push system

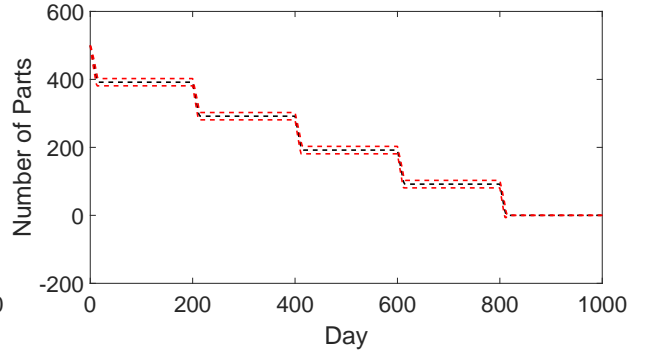
We use MLMC to compute the expected number of \mathcal{P}_8 , delivered in 300 days for the push system of supply chain. We consider 13 random parameters, i.e., λ_1 - λ_5 are the production rates of the processes 1-5, $x_1(t=0)$, $x_2(t=0)$, $x_3(t=0)$ are the initial inventories of \mathcal{P}_1 - \mathcal{P}_3 , $\hat{t}_i, i = 1, \dots, 5$ are the processing time of processes 1-5. The parameters are independently uniformly distributed as follows:

$$\begin{aligned} \lambda_1 &\sim \mathcal{U}(8, 12), \quad \lambda_2 \sim \mathcal{U}(8, 12), \quad \lambda_3 \sim \mathcal{U}(4, 6), \quad \lambda_4 \sim \mathcal{U}(8, 12), \quad \lambda_5 \sim \mathcal{U}(1, 3), \\ x_1(t=0) &\sim \mathcal{U}(800, 1200), \quad x_2(t=0) \sim \mathcal{U}(300, 700), \quad x_3(t=0) \sim \mathcal{U}(800, 1200), \\ \hat{t}_1 &\sim \mathcal{U}(1, 2), \quad \hat{t}_2 \sim \mathcal{U}(1, 2), \quad \hat{t}_3 \sim \mathcal{U}(10, 20), \quad \hat{t}_4 \sim \mathcal{U}(1, 2), \quad \hat{t}_5 \sim \mathcal{U}(10, 50). \end{aligned}$$

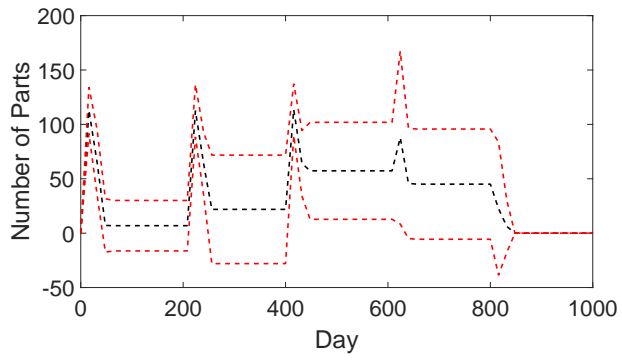
We evenly split the total tolerance on the bias and statistical error, i.e., $\epsilon_b^2 = 0.5TOL^2$ $\epsilon_s^2 = 0.5TOL^2$. The estimated values of a , b and g are 1.5, 2 and 1, respectively. We show the numbers of samples in Table



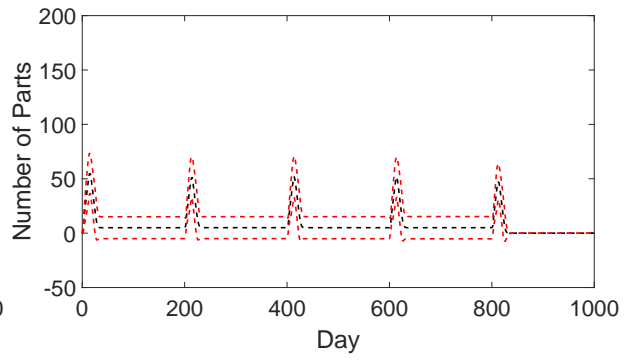
(a)



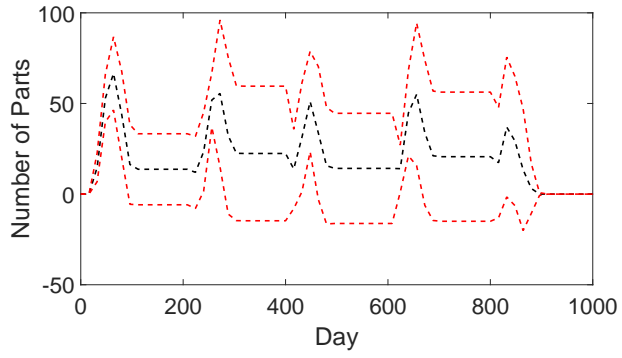
(b)



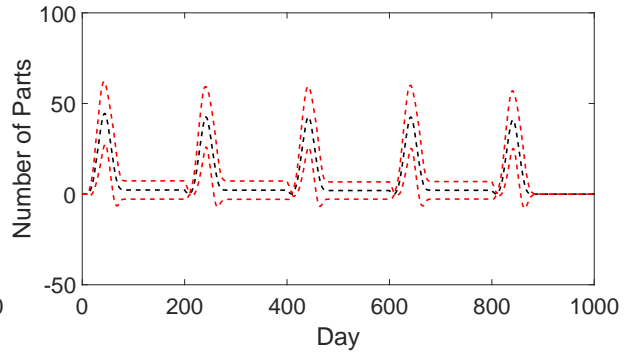
(c)



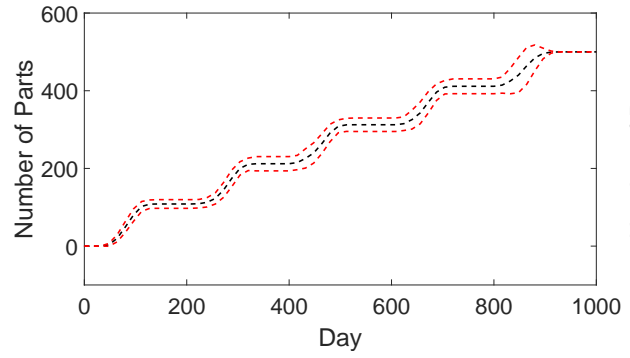
(d)



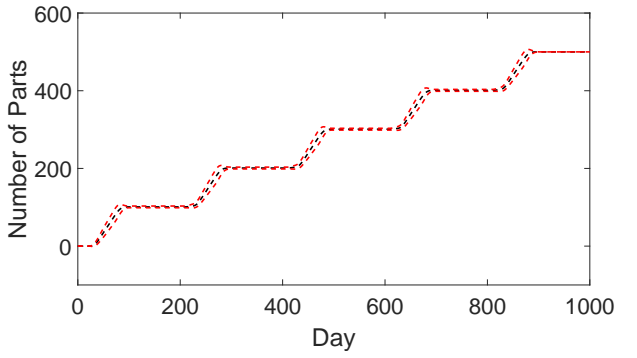
(e)



(f)



(g)



(h)

Figure 11: Stochastic pull system. $\Delta t = 16$ days: (a) \mathcal{P}_2 (c) \mathcal{P}_4 (e) \mathcal{P}_6 (g) \mathcal{P}_8 ; $\Delta t = 2$ days: (b) \mathcal{P}_2 (d) \mathcal{P}_4 (f) \mathcal{P}_6 (h) \mathcal{P}_8

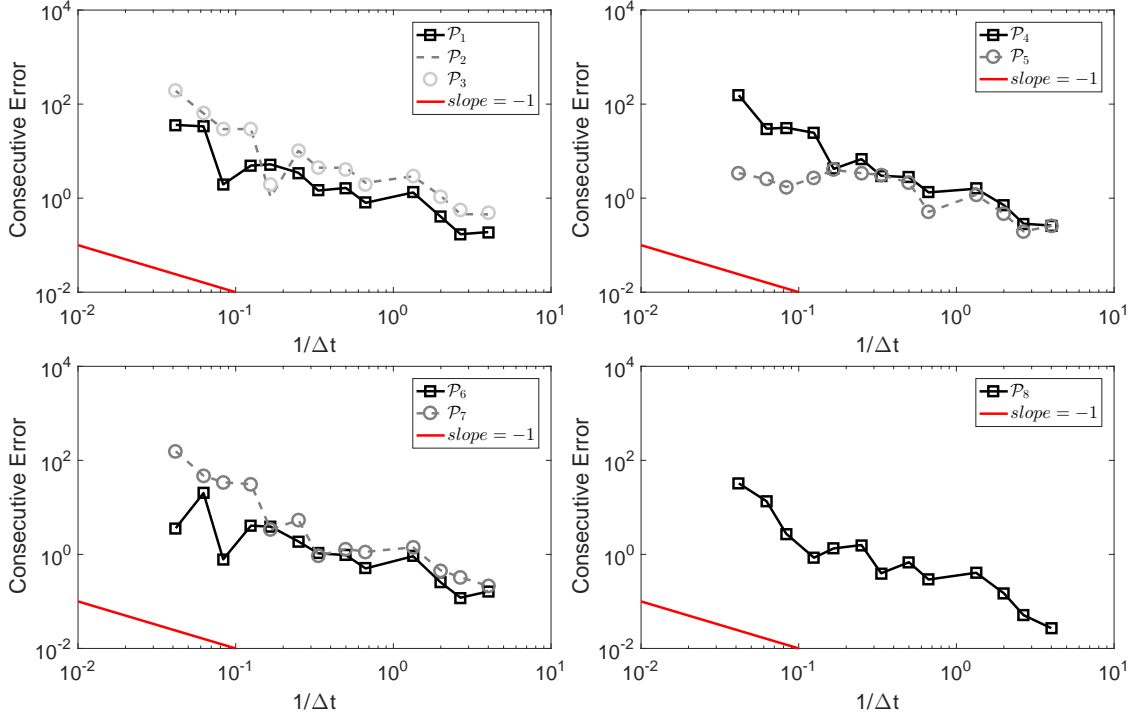


Figure 12: Stochastic pull system. The consecutive errors of the quantities of the parts on the 730th day w.r.t. the time discretization.

1. The number of required levels commonly increases as we decrease the tolerance. Nevertheless, note that we have over-killed the bias when the tolerances are set to be 2.5% and 0.5%, consequently, the number of levels does not change when the tolerance decreases to 1.25% and 0.25% respectively.

The results and costs of the MLMC estimator are listed in Table 2. It is shown that we achieved 3.27 times acceleration when tolerance is 30(7.5%), 7 times acceleration when the tolerances are 10(2.5%) and 5(1.25%), 70 times acceleration when the tolerances are 2(0.5%) and 1(0.25%). The relative tolerance is shown in the parentheses of the first column.

5.5. Uncertainty propagation using MLMC - pull system

In the last example, we consider both parametric and stochastic uncertainties for the pull system in 5.3. We vary in total 23 parameters in the system. λ_1 - λ_5 are the average production rates of the corresponding processes 1-5, λ_6 - λ_{10} are the mean transportation rates associated with the processes 6-10, $x_1(t=0)$, $x_2(t=0)$, $x_3(t=0)$ are the initial inventories of \mathcal{P}_1 - \mathcal{P}_3 , $\hat{t}_i, i=1, \dots, 5$ are the processing time of processes 1-5, $\hat{t}_i, i=6, \dots, 10$ are the transportation delays in the processes 6-10. The parameters are independently uniformly distributed as follows:

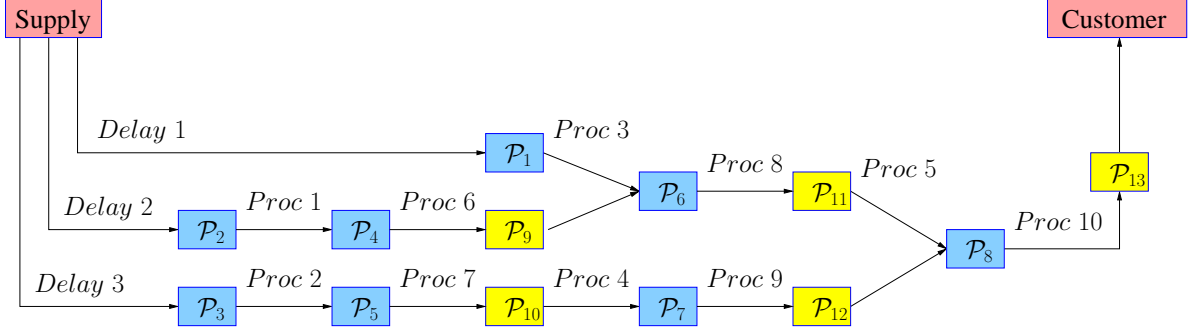


Figure 13: A modified manufacturing system which includes transportation.

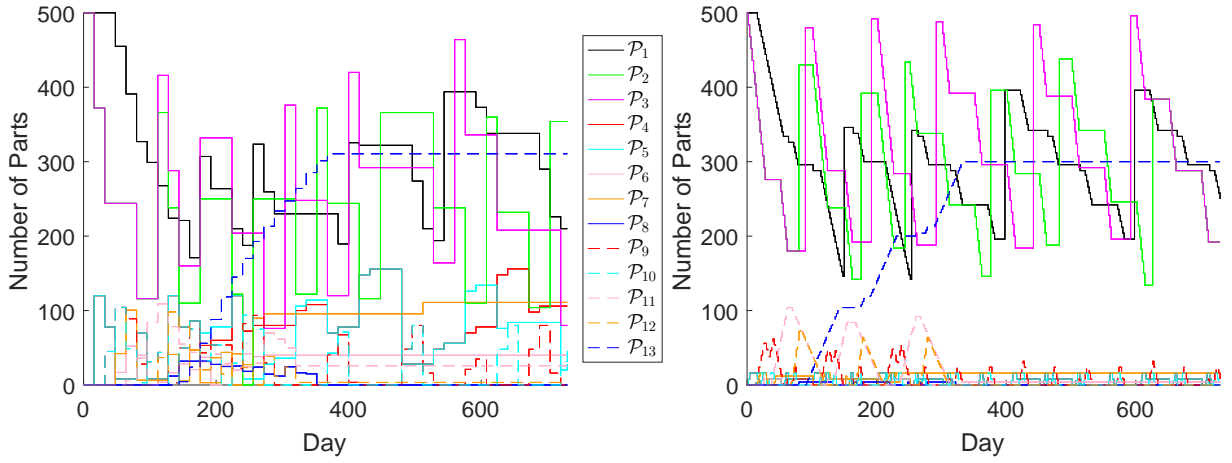
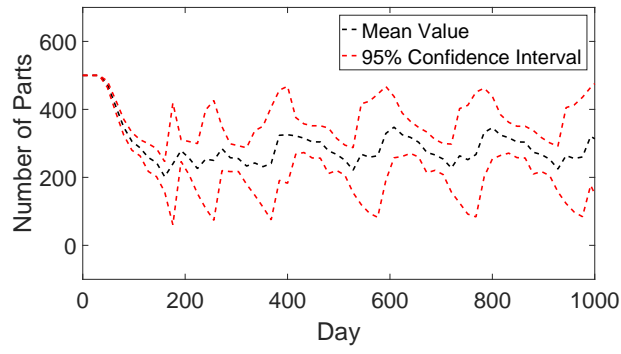


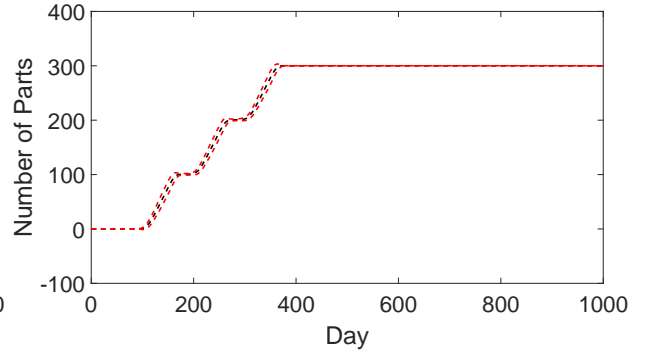
Figure 14: The time history of the state vector in the complex pull system with transportation. From left to right, the trajectories are simulated using time buckets $\Delta t = 16$ days and $\Delta t = 2$ days, respectively.

$$\begin{aligned}
\lambda_1 &\sim \mathcal{U}(8, 12), \quad \lambda_2 \sim \mathcal{U}(8, 12), \quad \lambda_3 \sim \mathcal{U}(4, 6), \quad \lambda_4 \sim \mathcal{U}(8, 12), \quad \lambda_5 \sim \mathcal{U}(1, 3), \\
\lambda_6 &\sim \mathcal{U}(7, 9), \quad \lambda_7 \sim \mathcal{U}(7, 9), \quad \lambda_8 \sim \mathcal{U}(7, 9), \quad \lambda_9 \sim \mathcal{U}(7, 9), \quad \lambda_{10} \sim \mathcal{U}(1, 2), \\
x_1(t=0) &\sim \mathcal{U}(800, 1200), \quad x_2(t=0) \sim \mathcal{U}(300, 700), \quad x_3(t=0) \sim \mathcal{U}(800, 1200), \\
\hat{t}_1 &\sim \mathcal{U}(1, 2), \quad \hat{t}_2 \sim \mathcal{U}(1, 2), \quad \hat{t}_3 \sim \mathcal{U}(10, 20), \quad \hat{t}_4 \sim \mathcal{U}(1, 2), \quad \hat{t}_5 \sim \mathcal{U}(10, 50), \\
\hat{t}_6 &\sim \mathcal{U}(8, 12), \quad \hat{t}_7 \sim \mathcal{U}(8, 12), \quad \hat{t}_8 \sim \mathcal{U}(8, 12), \quad \hat{t}_9 \sim \mathcal{U}(40, 60), \quad \hat{t}_{10} \sim \mathcal{U}(8, 12),
\end{aligned}$$

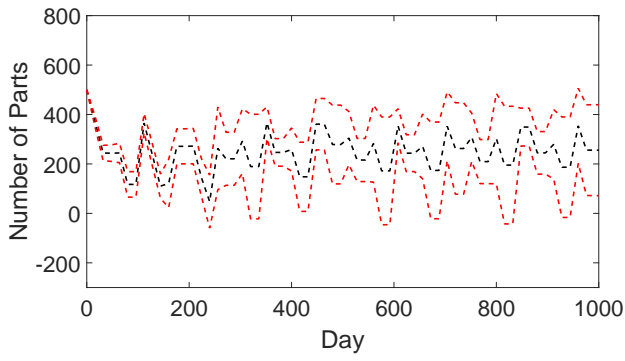
We impose repetitive final product orders (100 quantities per order) with 100 days' intervals. We also impose spare-part orders for parts 4, 5, 6 and 7: 30 parts per order, every 30 days. We evenly split the total tolerance on the bias and statistical error, i.e., $\epsilon_b^2 = 0.5TOL^2$, $\epsilon_s^2 = 0.5TOL^2$. Under parametric uncertainties, the expected number of delivery of the final products in 3650 days are shown in the left picture of Figure 16, where the MLMC simulation are repeated 20 times for four different values of the tolerances, i.e., 1, 2, 5 and 10. The mean value converges to 3560 as we decreases the tolerances, while the variability of the estimator is



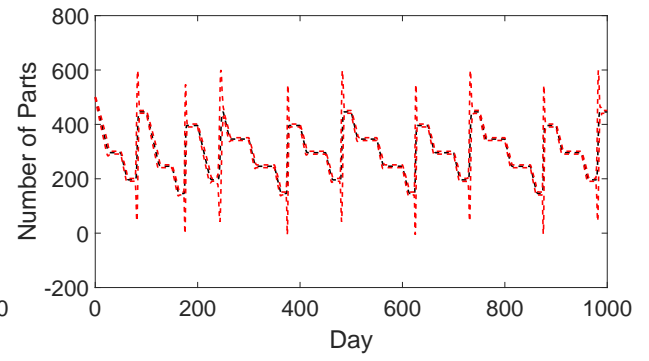
(a)



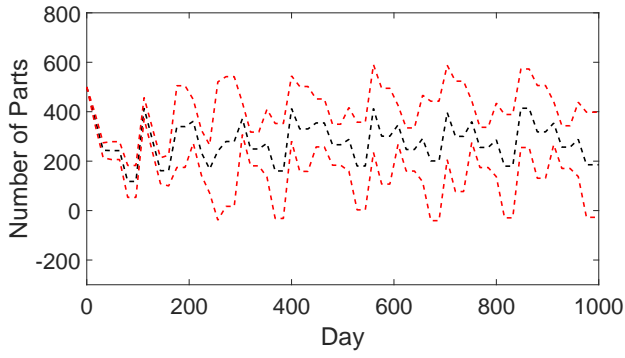
(b)



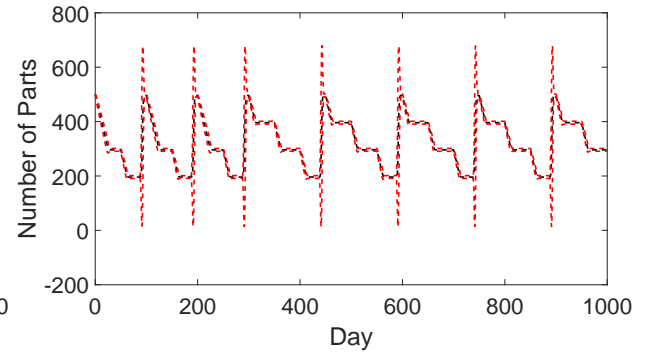
(c)



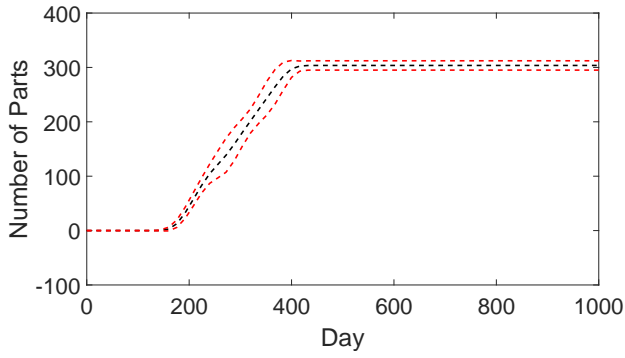
(d)



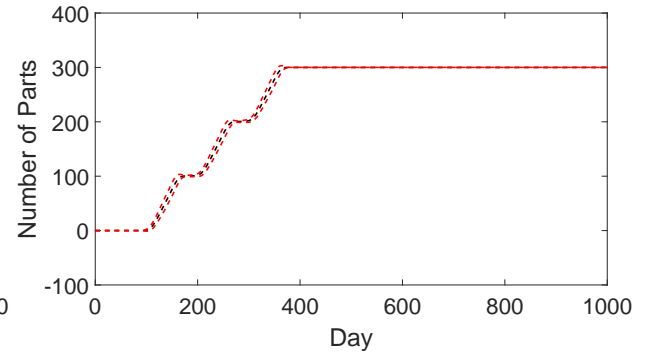
(e)



(f)



(g)



(h)

Figure 15: Stochastic pull system with both orders and transportation. $\Delta t = 16$ days: (a) \mathcal{P}_1 (c) \mathcal{P}_2 (e) \mathcal{P}_4 (g) \mathcal{P}_{13} ; $\Delta t = 0.5$ days: (b) \mathcal{P}_1 (d) \mathcal{P}_2 (f) \mathcal{P}_3 (h) \mathcal{P}_{13}

tightly controlled by the prescribed tolerances. The right picture of Figure 16 compares the computational time of the MLMC with standard MC. It is note-worthy that the MLMC can be several magnitudes more efficient than standard MC as it has a much smaller rate of growth w.r.t. the tolerance.

We furthermore compute the expected delivery time of 500 final products: $\mathbf{E}(\min(t)|x_8(t) \geq 500)$. The left picture in Figure 17 shows 20 batches of MLMC simulations of the expected delivery time for four different values of the tolerances, i.e., 0.5, 1, 2 and 4 days. The mean value converges to 584 days, while we also observe that the variability of the MLMC results are controlled rigorously by the tolerance. The right picture of Figure 17 compares the computational time of the MLMC estimator with the standard MC. Again, the MLMC estimator is several magnitudes faster than standard MC. More specifically, it is 10 times faster than MC when the tolerance is 4 days. This factor grows to 100 as we reduce the tolerance to 0.5 days.

Finally, we consider both parametric and stochastic uncertainties, the numbers of consumed parts and produced parts are assumed to follow Poisson and Binomial distributions of (10) and (11), respectively. We compute the expectation of the delivery time of 300 final products, i.e., $\mathbf{E}(\min(t)|x_{13}(t) \geq 300)$, using MLMC. $\Delta t = 5$ days on the coarsest level. The left picture of Figure 18 shows the results of 20 runs of MLMC against the tolerances. The average delivery time converges to 393.6 days. The right picture of Figure 18 shows the average computational costs of the MLMC estimator w.r.t. the tolerances. For tolerance smaller than 1, the MLMC is significantly advantageous to the standard MC as the multilevel complexity grows much slower than the MC. The reference rate of MLMC ϵ^{-2} ($a = 1.24$, $b = 1.07$, $g = 0.97$) is similarly to the growth of CPU time.

6. Conclusion

We presented a time bucket method to approximate DES for supply chains. The method is much faster than DES and led to the same results as the DES when the time bucket becomes small. The stochastic time bucket method for supply chains (L-leap method) is an extension of the D-leap method [3]. The new method incorporates several essential features for supply chain simulations, for example, limited capacities, push and pull productions, transportation, inventory refilling, and priority productions. The time buckets naturally offer a hierarchy of models which can be combined with MLMC to accelerate the propagation of uncertainties in a supply chain network. We showed more than 10 times speed up using our approach compared to standard MC using various examples. Considering future work, we note that the framework of combining time buckets and MLMC can be applied to the agent-based [30] and continuous modeling [10] of supply chains to achieve efficient uncertainty propagation.

Tol (percentage)	level 0	level 1	level 2	level 3	level 4	level 5	level 6	level 7	level 8
1 (0.25%)	48610	13071	4248	1720	617	189	61	28	15
2 (0.5%)	11872	3110	1085	441	164	53	16	6	2
5 (1.25%)	1700	459	145	58	21	7			
10 (2.5%)	376	103	35	14	5	2			
30 (7.5%)	43	15	5	2	1				

Table 1: Number of samples associated with different levels in MLMC given the tolerance.

Tol (percentage)	result	MLMC cost (second)	MC cost (second)
1 (0.25%)	401	33.9	2470
2 (0.5%)	404	8.1	615
5 (1.25%)	402	1.1	7.5
10 (2.5%)	414	0.24	1.7
30 (7.5%)	396	0.034	0.11

Table 2: The results and cost of MLMC compared to standard MC.

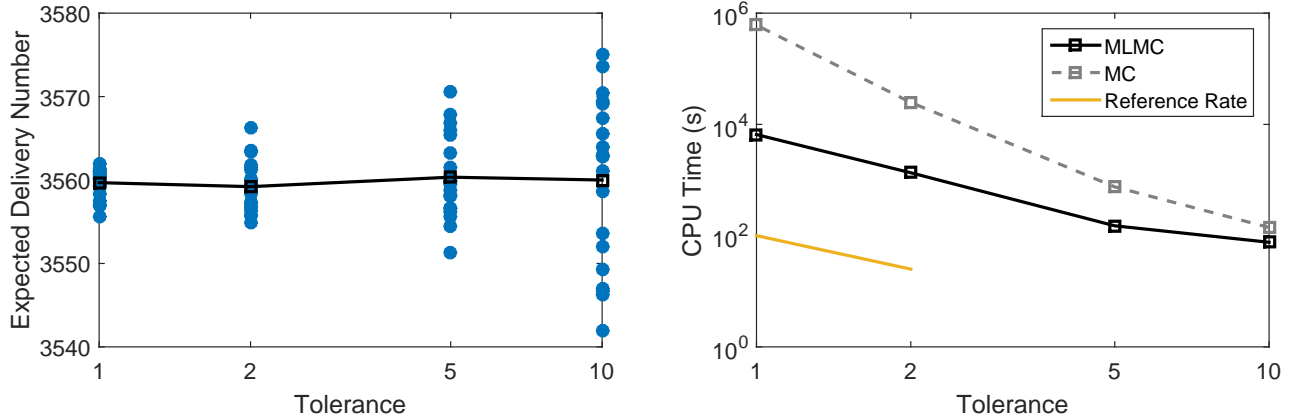


Figure 16: The left figure shows the expected delivery of the final product in 3650 days in example 5.5; The right figure shows the average computational cost of MLMC w.r.t. the numerical tolerances in example 5.5. The reference is computed using the MLMC theory in Section 4 ($a \approx 1.90$, $b \approx 0.78$, $g \approx 1.13$).

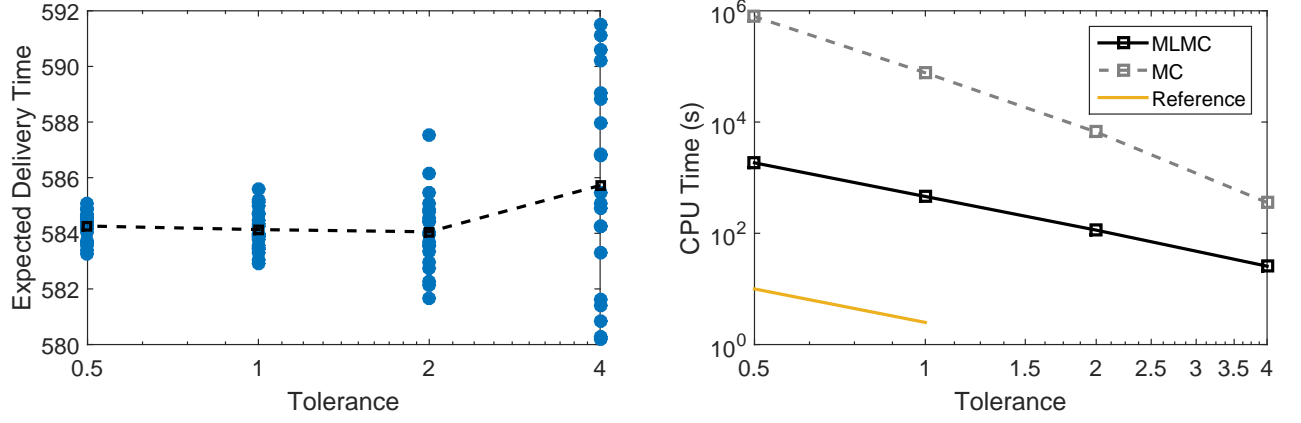


Figure 17: The left figure shows the expected delivery time of 500 products in example 5.4; The right figure shows the average computational cost of MLMC w.r.t. the numerical tolerances in example 5.5. The reference is computed using the MLMC theory in Section 4 ($a \approx 1.37$, $b \approx 1.44$, $g \approx 0.98$).

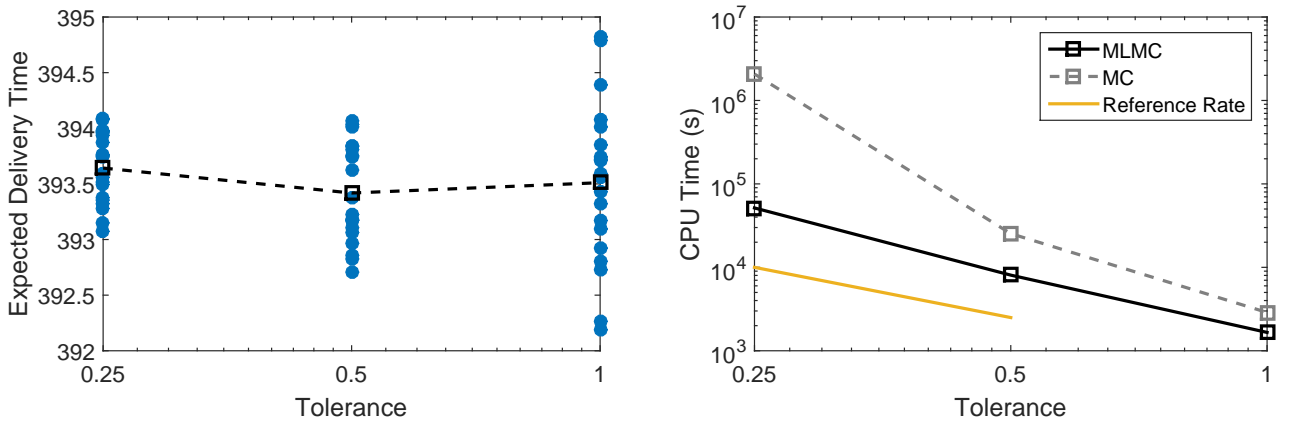


Figure 18: The left figure shows the expected delivery time of 300 final product in example 5.5; The right figure shows the average computational cost of MLMC w.r.t. the numerical tolerances in example 5.5. The reference is computed using the MLMC theory in Section 4 ($a \approx 1.24$, $b \approx 1.07$, $g \approx 0.97$).

7. Acknowledgment

The authors would like to acknowledge support from United Technologies Research Center through the innovation pipeline program and the capability program of the systems department. We thank Thomas Frewen for valuable proofreading.

References

- [1] Anderson, D. F., & Higham, D. J. (2012). Multilevel monte carlo for continuous time markov chains, with applications in biochemical kinetics. *Multiscale Modeling & Simulation*, 10, 146–179.
- [2] Baldwin, R. (2012). *Global supply chains: Why they emerged, why they matter, and where they are going*. CEPR Discussion Papers 9103 C.E.P.R. Discussion Papers.
- [3] Bayati, B., Chatelain, P., & Koumoutsakos, P. (2009). D-leaping: Accelerating stochastic simulation algorithms for reactions with delays. *Journal of Computational Physics*, 228, 5908 – 5916.
- [4] Beck, J., Dia, B. M., Espath, L. F., Long, Q., & Tempone, R. (2018). Fast Bayesian experimental design: Laplace-based importance sampling for the expected information gain. *Computer Methods in Applied Mechanics and Engineering*, 334, 523 – 553.
- [5] Bonney, M., Zhang, Z., Head, M., Tien, C., & Barson, R. (1999). Are push and pull systems really so different? *International Journal of Production Economics*, 59, 53–64.
- [6] Cao, Y., Gillespie, D. T., & Petzold, L. R. (2006). Efficient step size selection for the tau-leaping simulation method. *The Journal of Chemical Physics*, 124, 044109.
- [7] Chatterjee, A., Vlachos, D. G., & Katsoulakis, M. A. (2005). Binomial distribution based τ -leap accelerated stochastic simulation. *The Journal of Chemical Physics*, 122, 024112.
- [8] Collier, N., Haji-Ali, A.-L., Nobile, F., von Schwerin, E., & Tempone, R. (2015). A continuation multilevel monte carlo algorithm. *BIT Numerical Mathematics*, 55, 399–432.
- [9] Daniel, J. S. R., & Rajendran, C. (2005). A simulation-based genetic algorithm for inventory optimization in a serial supply chain. *International Transactions in Operational Research*, 12, 101–127.
- [10] d’Apice, C., Gottlich, S., Herty, M., & Piccoli, B. (2010). *Modeling, simulation, and optimization of supply chains: a continuous approach* volume 121. SIAM.
- [11] Fu, M. C., Bayraksan, G., Henderson, S. G., Nelson, B. L., Powell, W. B., Ryzhov, I. O., & Thengvall, B. (2014). Simulation optimization: A panel on the state of the art in research and practice. In *Simulation Conference (WSC), 2014 Winter* (pp. 3696–3706). IEEE.
- [12] Giles, M. B. (2008). Multilevel monte carlo path simulation. *Operations Research*, 56, 607–617.
- [13] Giles, M. B. (2015). Multilevel monte carlo methods. *Acta Numerica*, 24, 259–328.
- [14] Gillespie, D. T. (2001). Approximate accelerated stochastic simulation of chemically reacting systems. *The Journal of Chemical Physics*, 115, 1716–1733.
- [15] Grossmann, I. E. (2005). Enterprise-wide optimization: A new frontier in process systems engineering. *AIChE Journal*, 51, 1846–1857.
- [16] Jahangirian, M., Eldabi, T., Naseer, A., Stergioulas, L. K., & Young, T. (2010). Simulation in manufacturing and business: A review. *European Journal of Operational Research*, 203, 1 – 13.
- [17] Kapuscinski, R., & Tayur, S. (1999). Optimal policies and simulation-based optimization for capacitated production inventory systems. *Quantitative Models for Supply Chain Management*, (pp. 7–40).

- [18] Kleijnen, J. P. (2005). Supply chain simulation tools and techniques: a survey. *International Journal of Simulation and Process Modelling*, 1, 82–89.
- [19] Law, A. M. (2014). *Simulation Modeling and Analysis*. McGraw-Hill Higher Education.
- [20] Li, S. (1989). Marked event method in discrete event simulation. In *Proceedings of the 21st conference on Winter simulation* (pp. 719–728). ACM.
- [21] Lu, H., Liu, X., Pang, W., Ye, W. H., & Wei, B. S. (2012). Modeling and simulation of aircraft assembly line based on quest. In *Advanced Materials Research* (pp. 666–669). Trans Tech Publ volume 569.
- [22] Maravelias, C. T., & Grossmann, I. E. (2003). New general continuous-time statetask network formulation for short-term scheduling of multipurpose batch plants. *Industrial & Engineering Chemistry Research*, 42, 3056–3074.
- [23] Montevechi, J. A. B., de Pinho, A. F., Leal, F., & Marins, F. A. S. (2007). Application of design of experiments on the simulation of a process in an automotive industry. In *Proceedings of the 39th conference on Winter simulation: 40 years! The best is yet to come* (pp. 1601–1609). IEEE Press.
- [24] Moraes, A., Tempone, R., & Vilanova, P. (2014). Hybrid chernoff tau-leap. *Multiscale Modeling & Simulation*, 12, 581–615.
- [25] Moraes, A., Tempone, R., & Vilanova, P. (2016). Multilevel hybrid chernoff tau-leap. *BIT Numerical Mathematics*, 56, 189–239.
- [26] Rosenblatt, M. J., Roll, Y., & Vered Zyser, D. (1993). A combined optimization and simulation approach for designing automated storage/retrieval systems. *IIE Transactions*, 25, 40–50.
- [27] Shapiro, J. F. (2006). *Modeling the supply chain* volume 2. Cengage Learning.
- [28] Simatupang, T. M., & Sridharan, R. (2002). The collaborative supply chain. *The International Journal of Logistics Management*, 13, 15–30.
- [29] Stadtler, H. (2005). Supply chain management and advanced planning—basics, overview and challenges. *European Journal of Operational Research*, 163, 575–588.
- [30] Swaminathan, J. M., Smith, S. F., & Sadeh, N. M. (1998). Modeling supply chain dynamics: A multiagent approach. *Decision sciences*, 29, 607–632.
- [31] Thierry, C., Thomas, A., & Bel, G. (2008). *Simulation for Supply Chain Management*. Wiley.
- [32] Yan, Y., & Wang, G. (2007). A job shop scheduling approach based on simulation optimization. In *Industrial Engineering and Engineering Management, 2007 IEEE International Conference on* (pp. 1816–1822). IEEE.
- [33] You, F., & Grossmann, I. E. (2008). Mixed-integer nonlinear programming models and algorithms for large-scale supply chain design with stochastic inventory management. *Industrial & Engineering Chemistry Research*, 47, 7802–7817.
- [34] Ziarnetzky, T., Mönch, L., & Biele, A. (2014). Simulation of low-volume mixed model assembly lines: Modeling aspects and case study. In *Proceedings of the 2014 Winter Simulation Conference* (pp. 2101–2112). IEEE Press.